THE JOURNAL OF BIOLOGICAL CHEMISTRY
Vol. 271, No. 30, Issue of July 26, pp. 18007–18016, 1996
Printed in U.S.A.
© 1996 by The American Society for Biochemistry and Molecular Biology, Inc.

Lipase Activation by Nonionic Detergents

THE CRYSTAL STRUCTURE OF THE PORCINE LIPASE-COLIPASE-TETRAETHYLENE GLYCOL MONOOCTYL ETHER COMPLEX*

(Received for publication, November 27, 1995, and in revised form, April 12, 1996)

Juan Hermoso‡, David Pignol‡, Brigitte Kerfelec§, Isabelle Crenon§, Catherine Chapus§, and Juan Carlos Fontecilla-Camps‡¶

From the ‡Laboratoire de Cristallographie et de Cristallogénèse des Protéines, Institut de Biologie Structurale Jean-Pierre Ebel, CEA-CNRS, 41 Avenue des Martyrs, 38027 Grenoble Cedex 1, France and the §Laboratoire de Bioénergétique et d'Ingénierie des Protéines, UPR 9036 CNRS, BP71, 13402 Marseille Cédex 9, France

The crystal structure of the ternary porcine lipase-colipase-tetra ethylene glycol monooctyl ether (TGME) complex has been determined at 2.8 Å resolution. The crystals belong to the cubic space group F23 with *a* = 289.1 Å and display a strong pseudo-symmetry corresponding to a P23 lattice. Unexpectedly, the crystalline two-domain lipase is found in its open configuration. This indicates that in the presence of colipase, pure micelles of the nonionic detergent TGME are able to activate the enzyme; a process that includes the movement of an N-terminal domain loop (the flap). The effects of TGME and colipase have been confirmed by chemical modification of the active site serine residue using diisopropyl *p*-nitrophenylphosphate (E600). In addition, the presence of a TGME molecule tightly bound to the active site pocket shows that TGME acts as a substrate analog, thus possibly explaining the inhibitory effect of this nonionic detergent on emulsified substrate hydrolysis at submicellar concentrations. A comparison of the lipase-colipase interactions between our porcine complex and the human-porcine complex (van Tilbeurgh, H., Egloff, M.-P., Martinez, C., Rugani, N., Verger, R., and Cambillau, C. (1993) *Nature* 362, 814–820) indicates that except for one salt bridge interaction, they are conserved. Analysis of the superimposed complexes shows a 5.4° rotation on the relative position of the N-terminal domains excepting the flap that moves in a concerted fashion with the C-terminal domain. This flexibility may be important for the binding of the complex to the water-lipid interface.

Pancreatic lipase (triacylglycerol acylhydrolase, EC 3.1.1.3) plays a key role in dietary fat absorption in the intestine. It converts insoluble long chain triglycerides into more polar molecules that are able to cross the brush border membrane of enterocytes as mixed micelles with bile salts. Besides their role in triglyceride digestion through lipid emulsification and intestinal fat absorption, bile salts exert a strong inhibitory effect by preventing lipase adsorption through coating of the water-lipid interface (1). Lipase adsorption is a fundamental process because the enzyme catalyzes a heterogeneous reaction that involves an interfacial activation step. To counteract the inhibitory effect of bile salts, the pancreas secretes a small protein, colipase (molecular mass, 10 kDa), which anchors lipase to the bile salt-coated water-lipid interface in their presence (2, 3). Thus, lipolysis results from the combined effect of pancreatic lipase, colipase, and bile salts.

Pancreatic lipase is a single polypeptide chain of 50 kDa. This protein has been characterized in several species, and the amino acid sequences of the enzyme from pig, man, horse, rabbit, rat, guinea pig, and coypu (4–10) have been reported. In addition, related lipases (type 1 and 2) have been found in dog, rat man, guinea pig, and coypu (11–16) by screening pancreatic cDNA libraries. The localization and role of these related lipases is not clear.

Crystal structures of the human (17, 18) and equine (19) lipases have shown that the polypeptide chain is divided into two domains bearing specific functions. The N-terminal domain contains the catalytic triad (Ser^{152}-His^{263}-Asp^{176}) and is responsible for triglyceride hydrolysis. The C-terminal domain is involved in colipase binding as initially established from biochemical data (20, 21) and subsequently confirmed by crystallographic studies (18, 22–24).

It is known from amino acid sequence comparisons that colipases in general constitute a highly homologous family (10, 25–29). These proteins posses two topologically distinct sites, an interfacial binding site involving the tyrosine-rich region of the molecule (30) and a lipase binding site containing polar residues (31, 32). The crystal structure of porcine colipase complexed to human lipase (18, 22, 23) showed that the polypeptide chain forms four fingers protruding from a compact core held together by a network of five invariant disulfide bridges. The interfacial binding site appears to be located at the tips of the fingers, whereas the lipase binding site is on the opposite side of the molecule.

A specific feature of pancreatic lipase, when compared with other classical serine hydrolases, is that the catalytic site is inaccessible to substrate in solution. A structural basis for this inaccessibility has been obtained from the crystal structures of human lipase (17, 18) and the porcine colipase-human lipase complex (22, 23). These studies have shown that in the former structure, the enzyme adopts an inactive, closed conformation with a surface loop from the N-terminal domain (the flap) covering the active site, and that in the latter lipase has an active open conformation resulting from the repositioning of the flap (22). The motion of the flap makes the active site accessible to the substrate, simultaneously forming a functional oxyanion hole and generating the lipase interfacial binding site. So far, the open conformation has only been observed when lipase was co-crystallized with colipase and either bile

* This work was supported by the Commissariat à l'Energie Atomique, the Centre National de la Recherche Scientifique, and the Institut National de la Recherche Medicale. The costs of publication of this article were defrayed in part by the payment of page charges. This article must therefore be hereby marked "*advertisement*" in accordance with 18 U.S.C. Section 1734 solely to indicate this fact.

¶ To whom correspondence should be addressed. Tel.: 33-76-88-59-20; Fax: 33-76-88-51-22; E-mail: juan@lccp.ibs.fr.

salt/phospholipid (22) or βoG/C11[1] alkylphosphonate mixed micelles (24).

Here, we report the three-dimensional structure of the porcine lipase-colipase complex. From this structure we conclude that the presence of both pure nonionic detergent micelles and colipase induces the activation of lipase in the absence of substrate. This observation has been confirmed by biochemical experiments based on the reactivity of the catalytic serine residue to E600. The presence of a TGME molecule bound to the active site pocket may provide an explanation for the inhibitory effect of submicellar concentrations of nonionic detergents on emulsified triglyceride hydrolysis. In addition, a comparison of our natural complex to the human porcine complex has allowed us to 1) define a set of lipase-colipase interactions that are likely to be conserved among the various species and 2) provide a possible explanation for the existence of an unnatural salt bridge in the human-porcine complex. Finally, through superposition studies of the human-porcine and porcine complexes, we conclude that the lipase-colipase complex is composed of two more or less rigid regions connected by a hinge: one of the regions is formed by the N-terminal domain excluding the flap, and the other is formed by by C-terminal domain, colipase, and the flap.

EXPERIMENTAL PROCEDURES

Biochemical Experiments

Purification of Porcine Pancreatic Lipase and Colipase—Both proteins were purified from a delipidated acetonic pancreatic powder. The two isolipases (LA and LB) were purified according to the method of Lombardo *et al.* (33). Porcine colipase was purified according to Chapus *et al.* (34).

Activity Measurements—Lipase activity was titrimetrically determined at pH 7.5 and 25 °C using 0.11 M emulsified triacylbutyrylglycerol (tributyrin) in 1 mM Tris/HCl buffer containing 0.1 M NaCl, 5 mM $CaCl_2$. Under these conditions, the specific activity of purified lipase is 8000 units/mg. One unit corresponds to the release of 1.0 μmol of fatty acid/min.

Inhibition of Pancreatic Lipase by E600—The inhibition experiments were performed in 50 mM sodium acetate buffer, pH 6.0, containing 0.1 M NaCl. Porcine lipase, either alone or in the presence of detergent and/or porcine colipase was treated with 4 mM E600. The mixture was incubated at 25 °C, and aliquots were withdrawn from the mixture at various time intervals. The remaining lipase activity was measured as mentioned above.

X-ray Structure Determination

Crystallization—The porcine lipase-colipase complex was crystallized by the sitting drop vapor diffusion method (35) at 20 °C. Typically, a stock complex solution was prepared by mixing 10 μl of lipase and 7 μl of colipase solutions at 10 mg/ml each corresponding to a 1:3 molar ratio of lipase to colipase. A total of 12 different nonionic detergents were screened in crystallization experiments using ammonium sulfate as the precipitating agent. Suitable crystals were obtained by mixing 2 μl of complex solution with 2 μl of a reservoir solution containing 50 mM MES, pH 6.0, 0.5 M ammonium sulfate, and 15 mM TGME. Under these conditions, TGME is essential for crystallization.

Data Collection—Preliminary x-ray data were collected at room temperature on a Xentronics/Siemens X-1000 area detector diffractometer coupled to a Rigaku RU200 rotating anode x-ray generator equipped with a graphite monochromator and a 3×0.3 mm^2 focal spot size. Data to 4.0 Å resolution were processed with the XENGEN software package (36) in the cubic space group P23, with $a = 144.6$ Å and one molecule in the asymmetric unit. A second diffraction data set was collected with a synchrotron radiation source (LURE, W32 station) on a MAR-Research image plate system. Inspection of diffraction images using MOSFLM (37) indicated that indexing using the space group P23 predicted only half of the reflections present in the diffraction pattern. The unaccounted for reflections were in general much weaker, revealing a strong P23 pseudo-symmetry. Re-indexation of the diffraction spots using the space group F23 ($a = 289.1$ Å) predicted all the observed reflections and allowed for the integration of the data. The porcine lipase-colipase complex corresponds to the first macromolecular crystal structure ever reported in F23. The crystals have a V_m of 4.3 $Å^3$/D, which corresponds to approximately 70% solvent (38). A total of 42,501 unique reflections with $F > 0.0$, corresponding to 86% of all data expected at 2.8 Å resolution, were scaled with the CCP4 crystallographic package (39). The relatively low internal consistency of the data ($R_{sym} = 0.13$, defined as $\Sigma I(i) - \langle I \rangle / \Sigma I(i)$) is due to the systematically weak intensities (mean $I/\sigma(I) = 3.4$) resulting from the P23 pseudo-symmetry.

TABLE I
Final model and refinement statistics

Resolution limits (Å)	6–2.8
Final R-factor[a]	0.21
Final free R-factor (56)	0.29
Number of reflections used ($F > 2\sigma_F$)	33758
Number of non-hydrogen atoms	
Protein	8356
TGME	42
Carbohydrate	122
Mercaptoethanolate	8
Ca^{2+}	2
Solvent molecules	422
r.m.s. deviation from standard geometry	
Bond length (Å)	0.011
Bond angle (°)	1.49
Torsion angle (°)	27.22
Improper angle (°)	2.62

[a] R-factor = $(\ _hF_o - F_c)/\ _hF_o$

Structure Solution and Refinement—AMoRe, an integrated computer program package of molecular replacement programs (40), was used to solve the structure of the porcine complex applying the horse lipase structure (Ref. 19; Protein Data Bank code HPL) as the search model. Rotation and translation searches, carried out using a 4–12 Å resolution range, led to unique independent solutions for the two molecules of the asymmetric unit. The positions of these molecules were then refined in the same resolution range with the rigid body option of AMoRe (41). The resulting R-factor and the correlation value were 0.34 and 0.77, respectively. Amino acid sequence changes were incorporated with the program O (42) running on an ESV/20 (Evans & Sutherland, Utah, USA) computer graphics system. The partial model was initially refined using the simulated annealing and the energy minimization protocols of X-PLOR (43), followed by periodic inspections of electron density maps. Subsequently, the Cys^{238}-Cys^{262} segment and the loop comprising residues 77–86 were manually rebuilt. At this stage, inspection of the ($F_o - F_c$) electron density map around the C-terminal domain of both crystallographically independent lipases revealed strong features that were assigned to the colipase molecules. Subsequently, the three-dimensional model of colipase (23, Protein Data Bank entry 1LPB) was manually positioned in this electron density in an orientation that corresponded approximately to the one observed for the human-porcine complex (22). Based on the electron density map, two extra residues were added to the N-terminal region of colipase. Next, the lipase model was completed with a five sugar moeity connected to Asn^{167}, a TGME molecule in the active site and a putative mercaptoethanolate bound to Cys^{182}. This model, to which water molecules were progressively added, was then refined with X-PLOR using noncrystallographic symmetry restraints.

The crystallographic R-factor converged at a value of 0.21 for reflections between 6 and 2.8 Å resolution (Table I). The final model contains 8356 nonhydrogen protein atoms, two Ca^{2+} ions, 422 water molecules, two TGME molecules, two mercaptoethanolates, four *N*-acetylglucosamine, and six mannose residues and has good stereochemistry. The two complex molecules in the asymmetric unit are related by a noncrystallographic 2-fold symmetry axis. This axis is shifted by 2 Å in the *a* direction and 1 Å in the *c* direction relative to the position it would occupy as a crystallographic axis in the space group P23, thus explaining the pseudo-symmetry observed (see above). Superposition of the two molecules of the asymmetric unit leads to an r.m.s. deviation of 0.5 Å on the Cα positions. Because they are very similar, only molecule A will be used in the following discussion. The final coordinates have been deposited with the Brookhaven Protein Data Bank and will be released one year after publication (Protein Data Bank access code 1ETH).

[1] The abbreviations used are: βoG, octyl-β-D-glucopyranoside; NaTDC, taurodeoxycholic acid sodium salt; TGME, tetraethylene glycol monooctyl ether; E600, diisopropyl *p*-nitrophenylphosphate; r.m.s., root mean square; MES, 4-morpholineethanesulfonic acid.

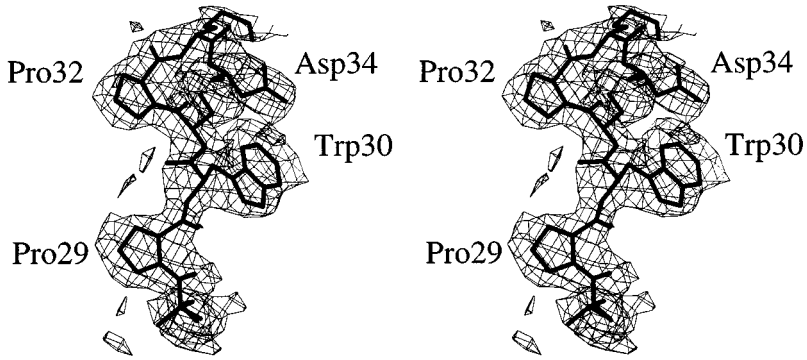

FIG. 1. **Stereo representation of the ($2F_o - F_c$) electron density map contoured at the 1 σ level, superimposed to the refined porcine lipase model.** In this region, the previously reported sequence (Pro[29]-Pro[30]-Asp[31]-Lys[32]) was modified according to the electron density map. The corrected sequence is indicated in the figure.

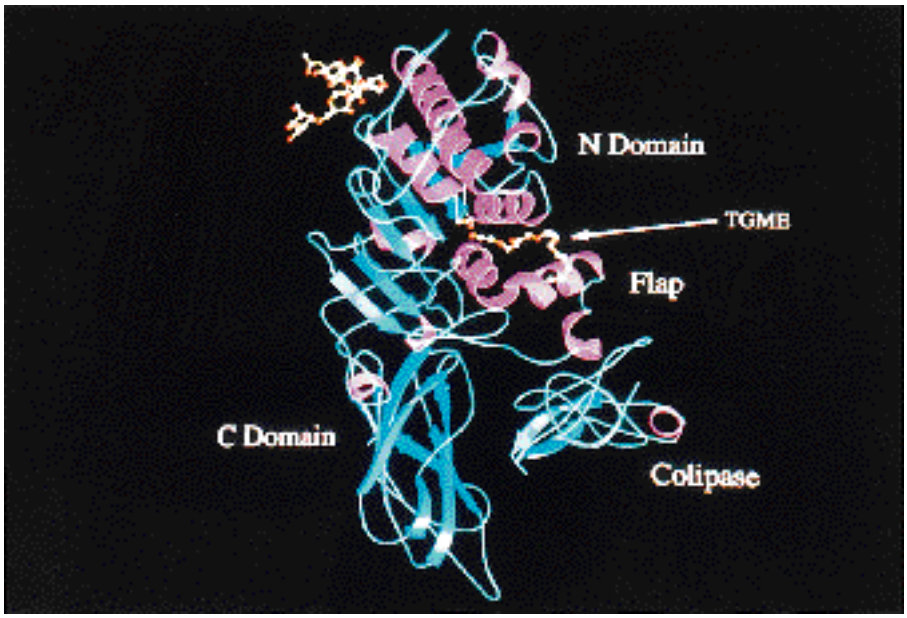

FIG. 2. **Schematic ribbon diagram of the porcine lipase-colipase structure.** The glycan chain, connected to the lipase N-terminal domain (*N Domain*), is drawn as a stick model. One TGME molecule, located in the open active site, is represented by *balls* and *sticks*. Colipase interacts with the lipase C-terminal domain (*C Domain*) and with the flap. The figure was made with the graphic program Molscript (57).

RESULTS

Structural Results

A Glycosylated "Open" Lipase—The refined structure clearly showed that the porcine lipase amino acid sequence previously reported (44) contained some errors. Inspection of the electron density map unambiguously revealed that positions 30, 31, and 32 corresponded to Trp, Ser, and Pro, respectively (Fig. 1). The presence of these residues has been confirmed by protein sequencing.[2] Thus, the previously reported sequence Pro[29]-Pro[30]-Asp[31]-Lys[32] has been now replaced by Pro[29]-Trp[30]-Ser[31]-Pro[32]-Lys[33], and the numbering of the complete chain has been adjusted to account for the inserted residue. In order to compare the results presented here with previously reported analyses, their numbering schemes should be shifted by adding one to residues past position 31.

The porcine lipase is a two-domain structure. The N-terminal domain is of the α/β type; it comprises residues 1–336 and contains the catalytic Ser[153], Asp[177], and His[264]. The C-terminal domain is a β-sandwich (45); it contains residues 337–449 and is responsible for most of the contacts with colipase. The overall structure of porcine lipase (Fig. 2) closely resembles those of the corresponding uncomplexed human (17) and horse (19) enzymes. The major difference is due to the conformation of the flap because a surface helix blocks the access to the catalytic triad in the latter two lipases. In the porcine complex reported here, lipase has an open conformation that is similar to the one described for the human-porcine complex (22): the Cys[238]-Cys[262] segment protrudes from the catalytic N-terminal domain and the 77–86 loop folds back onto the protein surface.

In the course of the refinement, ($F_o - F_c$) maps displayed a high electron density peak close to the Glu[188]-Asp[196] loop. Based on previous reports (17, 19), we assigned this peak to a Ca^{2+} ion that in our case, interacts with the highly conserved Glu[188], Arg[191], Asp[193], and Asp[196], forming a distorted square pyramid. The Ca^{2+} site, located far from the catalytic triad, is not likely to be directly involved in catalysis, and it appears to play a purely structural role in the loop.

Both porcine and human lipases are *N*-glycosylated at Asn[167] (46, 47). In the former, two isolipases A and B have been described differing both in the length (10 or 11 residues) (48) and in the branching organization of their glycan moieties (49). Two *N*-acetylglucosamines and three mannose (Man1–3) residues could be built into the corresponding electron density. From these studies, the crystalline porcine lipase was assigned unambiguously to isoform B, for which the carbohydrate chain bifurcates after the third sugar residue (Man[1]) into two distinct segments (Man[2] and Man[3]) (50).

The disulfide bridge pattern originally described for human lipase (17) is conserved in the porcine enzyme. A possible disulfide bridge interchange between Cys[91], Cys[102], and Cys[104] described for this enzyme (49) is not supported by our data: the free thiol group of Cys[104] is located 3.5 Å away from the S^{γ} atoms of the Cys[91]-Cys[102] disulfide bond (not shown). Porcine lipase has been reported to contain one free thiol group that is

[2] J. Bonicel, personal communication.

TABLE II
Lipase-colipase polar interactions

Conserved interactions in the porcine and human-porcine (22) complexes are indicated by bold characters.

Lipase	Colipase	Distances (Å)
Asn^{241} N	**Glu^{15} Oε2**	3.05
Ser^{244} Oγ	**Leu^{16} N**	3.05
Val^{247} O	**Arg^{38} NH1**	3.33
Asn^{366} Nδ2	**Glu^{45} O**	3.32
Gln^{369} N	**Glu^{64} Oε1**	2.76
Gln^{369} Nε2	**Arg^{65} O**	3.09
Lys^{400} Nz	**Glu^{45} Oε2**	2.73
Lys^{400} Nz	**Asn^{89} Oδ1**	3.19

TABLE III
Waters bridging interactions

Lipase	Distance (Å)	Water	Distances (Å)	Colipase
Asn^{366} O	2.6	Wat^{29}	2.6	Arg^{44} NH1
Asn^{366} N	2.8	Wat^{29}	2.8	Arg^{44} NH2
Gln^{369} O	3.11	Wat^{50}	2.8	Glu^{64} Oε2
Gln^{369} Oε1	3.14	Wat^{61}	3.7	Arg^{65} N

TABLE IV
van der Waals contacts

Conserved interactions in the porcine and human-porcine (22) complexes are indicated by bold characters.

Lipase	Colipase	Distances (Å)
Ser^{244} Cβ	Glu^{15} Cα	3.74
Leu^{243} Cδ1	Leu^{16} Cδ2	3.84
Ile^{249} Cγ2	Arg^{38} Cδ	3.9
Ile^{249} Cγ2	Arg^{38} CZ	3.26
Phe^{361} Cε2	**Glu^{45} Cδ**	3.56
Phe^{361} Cζ	**Glu^{45} Cδ**	3.65
Gln^{369} Cδ	Glu^{64} Cβ	3.85
Gln^{369} Cγ	Glu^{64} Cδ	3.72
Glu^{440} Cγ	Arg^{65} Cγ	3.57
Ile^{402} Cδ1	**Arg^{65} CZ**	3.49
Tyr^{404} Cγ	Arg^{65} CZ	3.78
Tyr^{404} Cδ2	Arg^{65} CZ	3.27
Tyr^{404} Cε2	**Arg^{65} Cγ**	3.63
Ile^{402} Cδ1	**Arg^{65} C**	3.65
Ile^{402} Cδ1	Gly^{66} Cα	3.65
Leu^{442} Cβ	Asn^{89} Cγ	3.64
Leu^{442} Cδ1	Asn^{89} Cγ	3.67

reactive toward sulfhydryl reagents (51); our structural results assign this reactivity to Cys^{182}, which we have modelled as a Cys residue modified by reaction with a β-mercaptoethanol molecule (see "Experimental Procedures").

Lipase-Colipase Interactions—Colipase is a flattened molecule that contains a cysteine-rich core and four hydrophobic fingers comprising segments 14–24, 27–39, 47–64,and 68–90. Its structure is very similar to the one described by Egloff *et al.* (23), although it seems to be slightly better ordered, because two additional N-terminal amino acids are seen in the electron density map. Despite the lack of regular secondary structure, colipase has an averaged temperature factor of 29.2 Å^2, which is similar to the one obtained for lipase (27.0 Å^2). The B factors reach a maximum of 35.0 Å^2 at the tips of the four fingers, reflecting the higher mobility of this region.

Porcine lipase and colipase interact through 8 polar, 17 van der Waals, and 4 water-mediated contacts (Tables II, III, and IV). Five of the polar contacts occur between colipase and the lipase C-terminal domain and the remaining three link colipase to the flap. These interactions are conserved in the human-porcine complex (22, 23), and according to amino acid comparisons they should be common to all lipase-colipase complexes. The only major difference between the two complexes at the lipase-colipase interface is the salt bridge between Arg^{44} of porcine colipase and Asp^{390} of human lipase, which is absent from the natural porcine complex (Fig. 3).

In order to determine the relative orientations of the N- and C-terminal domains of lipase in the porcine and human-porcine complexes, we carried out partial superposition studies. For the C-terminal domains of the two lipases the superposition resulted in an r.m.s. deviation of 0.58 Å in Cα positions for these regions (Fig. 4). The resulting orientations of the flap region and colipase were also very similar, with Cα r.m.s. deviations of 0.7 Å. In contrast, the positions of the N-terminal domains, excluding the flap region, were quite different, with r.m.s. deviations of 2.24 Å in the Cα positions. When the superposition of the two complexes was based on the N-terminal domains, a Cα r.m.s. deviation of 0.6 Å was obtained for these regions, indicating that they have very similar structures. The r.m.s. deviations of 2.24 Å in the Cα positions, observed in the first superposition, result from a 5.4 ° rotation of the N-terminal domain, excluding the flap, around residues Ser^{334} and Asn^{335}. These two residues present highly significant differences in the φ and Ψ torsion angle values between the porcine and human-porcine complexes ($\Delta\varphi = -46.23°$ and $\Delta\Psi = -115.33°$ for Ser^{334} and $\Delta\varphi = 166.57°$ and $\Delta\Psi = 57°$ for Asn^{335}). We conclude from these studies that the lipase-colipase complex is formed by two rigid units connected by a hinge region: one unit is formed by the C-terminal domain of lipase, colipase, and the flap region, and the other is formed by the lipase N-terminal domain, excluding the flap.

The Lipase Active Site—During refinement, the ($F_o - F_c$) Fourier maps consistently displayed a high electron density peak in the hydrophobic canyon of the open active site. Because neither inhibitors nor substrate were used in the crystallization experiments, it was concluded that the peak corresponded to a TGME molecule. Subsequently, the detergent molecule was modelled into the density with a double conformation, and the resulting ternary complex was refined to convergence (Fig. 5). The two conformers were assigned occupancies of 0.67 and 0.33, respectively, based on electron density peak heights and temperature factor values.

In both conformations of the TGME molecule, the aliphatic chain (from C-1 to C-8) is exposed to the solvent, whereas the hydrophilic moiety (from O-8 to O-16) is completely buried in the canyon of the lipase active site pocket (Fig. 6). The hydrophilic extremity of TGME presents two different types of interactions with lipase: in one conformer, O-16 is hydrogen-bonded to Ser^{153} of the catalytic triad, whereas in the other O-16 is hydrogen-bonded to Gly^{77} and Trp^{86}. In addition, there are six van der Waals interactions with residues forming the substrate cavity (Fig. 7). The stability of the TGME molecule in the active site is confirmed by its averaged B factor of 21.7 Å^2, lower than the corresponding value for the protein molecule, which is 27.6 Å^2. Due to the presence of the detergent, the orientation of the His^{264} ring, a member of the catalytic triad, differs significantly from the one found in the other open and closed lipase structures (Fig. 8).

The presence of a well stabilized TGME molecule in the active site and the open flap conformation of lipase in the porcine complex could correspond to either an artifact of the crystallization experiment or a specific effect of this detergent on lipase activation. In order to clarify this point, we have studied 1) the effects of the nonionic detergents on lipase activation through the reactivity of the catalytic serine residue to E600, a specific covalent inhibitor of serine proteases, and 2) the influence of nonionic detergents on emulsified terbutyrin hydrolysis.

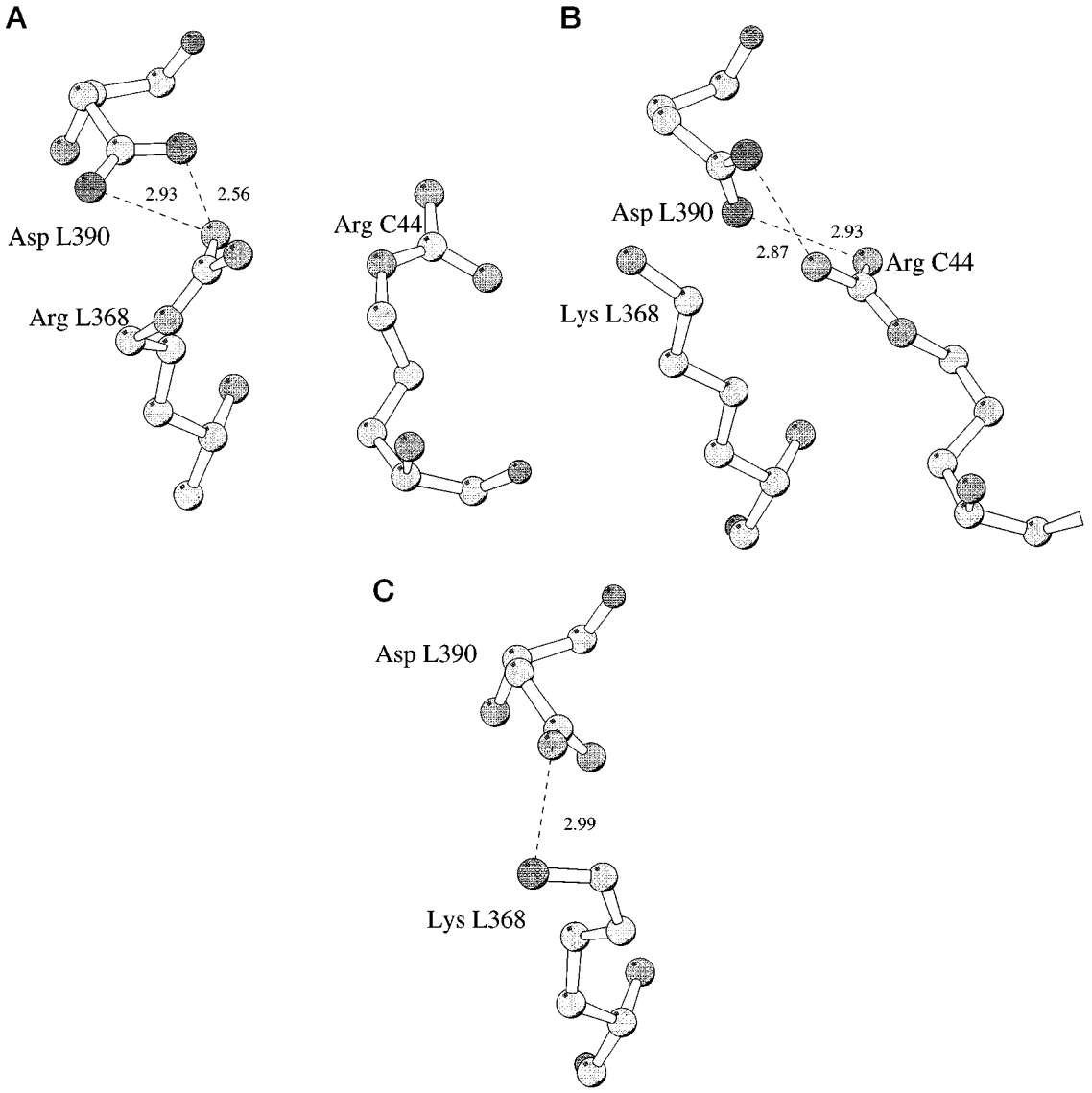

FIG. 3. **Molscript drawing (57) of Asp[390] and the basic residue at position 368 (lipase) the natural porcine complex (*a*), the human-porcine complex (*b*), and the uncomplexed human lipase (*c*).** In addition, Arg[44] (colipase) is depicted in *a* and *b*. Prefixes *L* and *C* denote residues coming from lipase and colipase, respectively.

Biochemical Results

Influence of Nonionic Detergents and Colipase on Lipase Inhibition by E600—E600 has been shown to inhibit pancreatic lipase irreversibly in the presence of colipase and micellar concentrations of NaTDC by reacting with the serine residue at the active site (52, 53). This result indicates that the combined effect of NaTDC micelles and colipase is to open the lipase flap, thereby making the active site serine residue accessible to inhibition. In order to investigate whether a similar effect could be induced by nonionic detergents, the enzyme was incubated with the E600 inhibitor in the presence of either TGME or βoG with and without colipase. As shown in Fig. 9 (*A* and *B*), lipase inhibition by E600 required supramicellar concentrations of the nonionic detergents in the presence of colipase. In the absence of colipase, lipase inhibition by E600 was not observed, even when supramicellar concentrations of the detergents were used (not shown). The extent of E600 inhibition in the presence of supramicellar concentrations of detergent was directly proportional to the colipase/lipase molar ratio (Fig. 10). As expected, full inhibition was reached for a 1:1 molar ratio. Thus, in the presence of colipase, both nonionic detergents and ionic ones are able to induce the conversion of lipase from a closed to an open conformation. Under the conditions used for the crystallization of the porcine complex (see "Experimental Procedures"), lipase was fully inhibited by E600 (not shown).

The opening of the flap by detergent micelles is a reversible phenomenon; a solution of lipase (10^{-4} M) incubated with colipase (2×10^{-4} M) and micelles of TGME (15 mM) in a 50 mM acetate buffer, pH 6.0, was completely inhibited by E600 (4 mM) within 30 min. However, when this solution was previously dialyzed 4 h at 0 °C against acetate buffer, there was no inhibition of lipase activity even 6 h after E600 addition. This indicates that lipase reverted to a closed conformation as a result of the removal of detergent micelles by dialysis.

Influence of Nonionic Detergents on Lipase Activity—The effect of the nonionic detergents TGME and βoG on lipase activity was tested both in the presence and the absence of colipase and compared with the effect of NaTDC, an ionic detergent.

In the absence of colipase, NaTDC (54), TGME, and βoG have a similar influence on lipase activity (Fig. 11). At very low (submicellar) detergent concentrations the three molecules en-

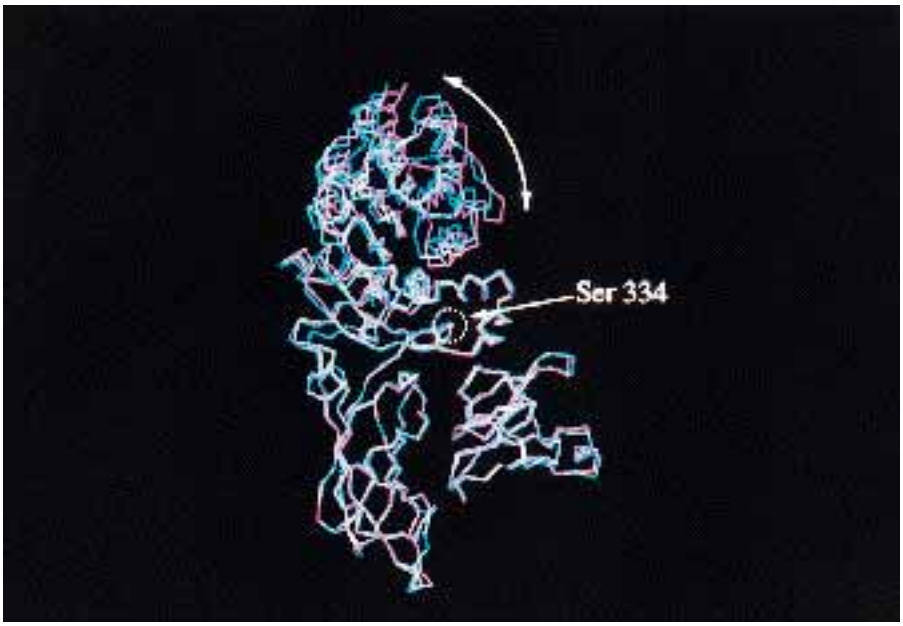

FIG. 4. **Superimposition of the porcine lipase-porcine colipase complex (*pink*) on the human lipase-porcine colipase complex (*blue*) (22).** The figure was made with the graphics program O (41).

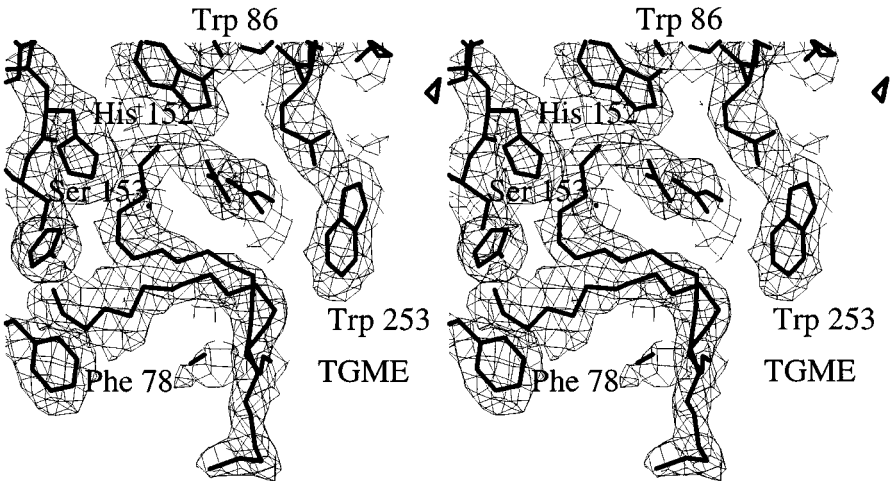

FIG. 5. **Representation of the ($2F_o - F_c$) electron density map superimposed to the TGME molecule (with the double conformation) and to the active site of lipase.** The electron density map was contoured at the 1 σ level. The lowest occupied conformer is the one on the *upper center* (see text).

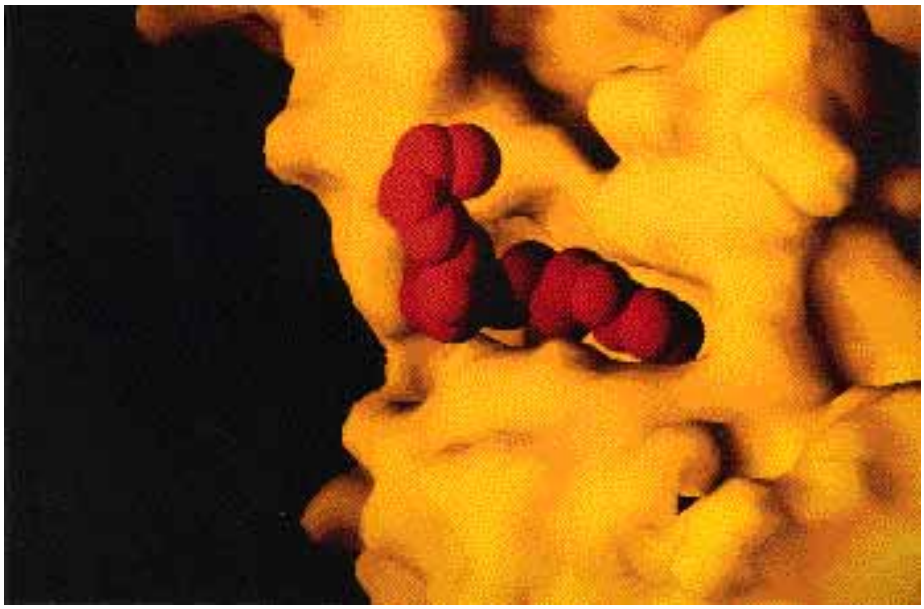

FIG. 6. **Complementarity between the nonionic detergent molecule and the hydrophobic cavity of the lipase active site.** The TGME molecule is shown as a CPK model (only the conformation of the molecule with the higher crystallographic occupancy (0.67) is depicted). The figure was made with the program GRASP (58).

hanced emulsified tributyrin hydrolysis, probably through substrate emulsion stabilization. In all cases, a subsequent increase in detergent concentration led to strong inhibition of lipase activity. Similar results have already been obtained with other nonionic detergents such as Triton X-100 and Nonipol TD-12 (54). The inhibition was complete for detergent concen-

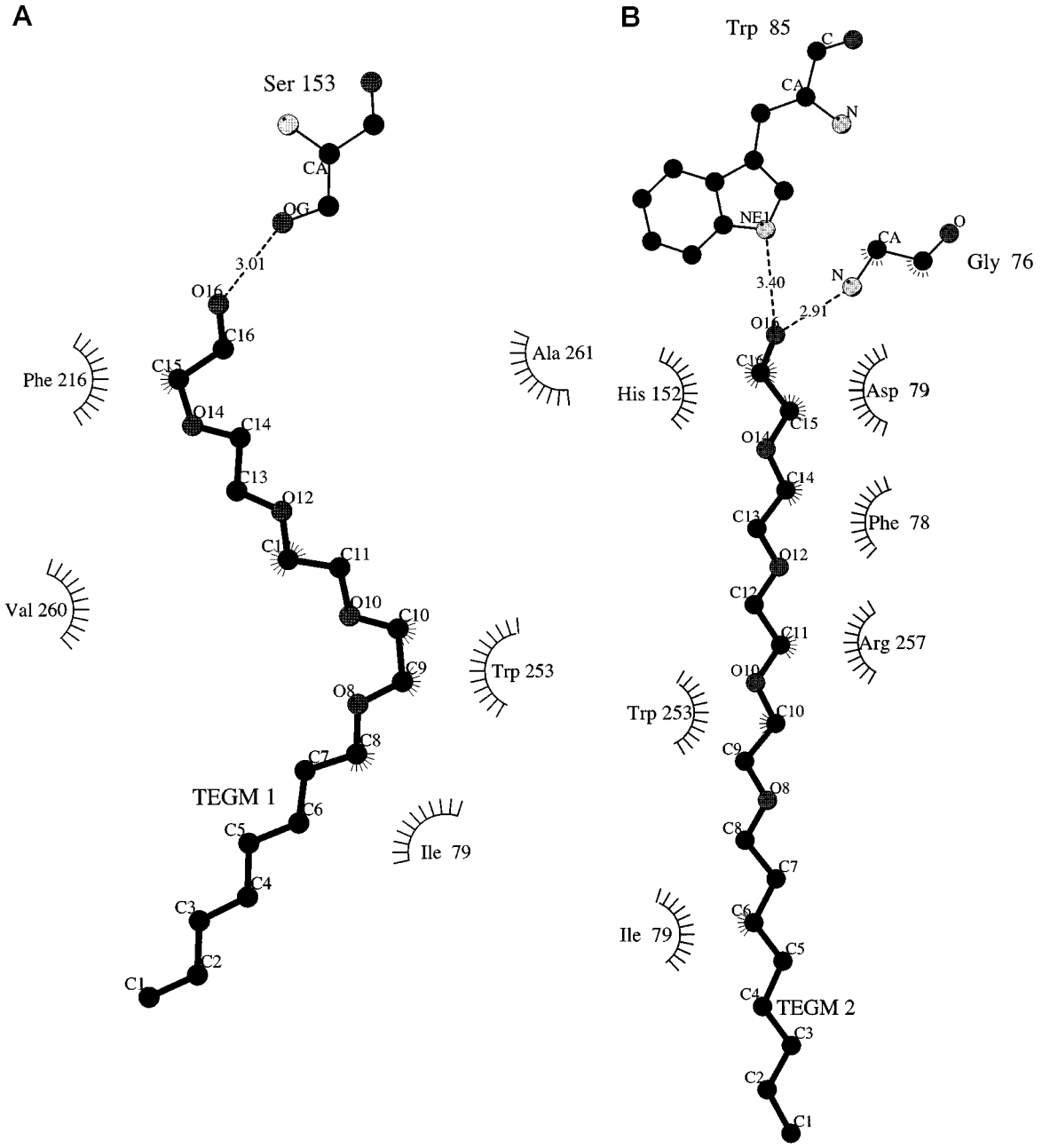

FIG. 7. **Schematic representation of the stabilization for conformer 1 (*a*) and conformer 2 of the TGME molecule (*b*).** This figure was made with the program LIGPLOT (59). Spiked residues form van der Waals contacts with the inhibitor.

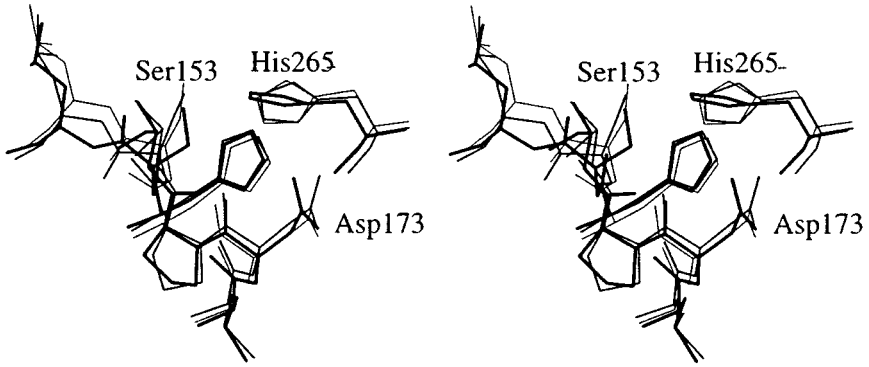

FIG. 8. **Stereo view of the catalytic triad (Ser^{153}, His^{264}, and Asp^{177}) in the open porcine (*thick line*), open human (*thin line*), and closed horse lipase structures.** The overall positions of the three residues are conserved in the three enzymes. Only the His^{264} ring presents a significantly different orientation in the porcine enzyme.

trations well below their critical micellar concentrations as measured in a 0.1 M NaCl solution (1, 7, and 25 mM for NaTDC, TGME, and βoG, respectively). It should be pointed out, however, that the critical micellar concentration values may shift downwards in the presence of a water-lipid interface due to the adsorption of detergent molecules.

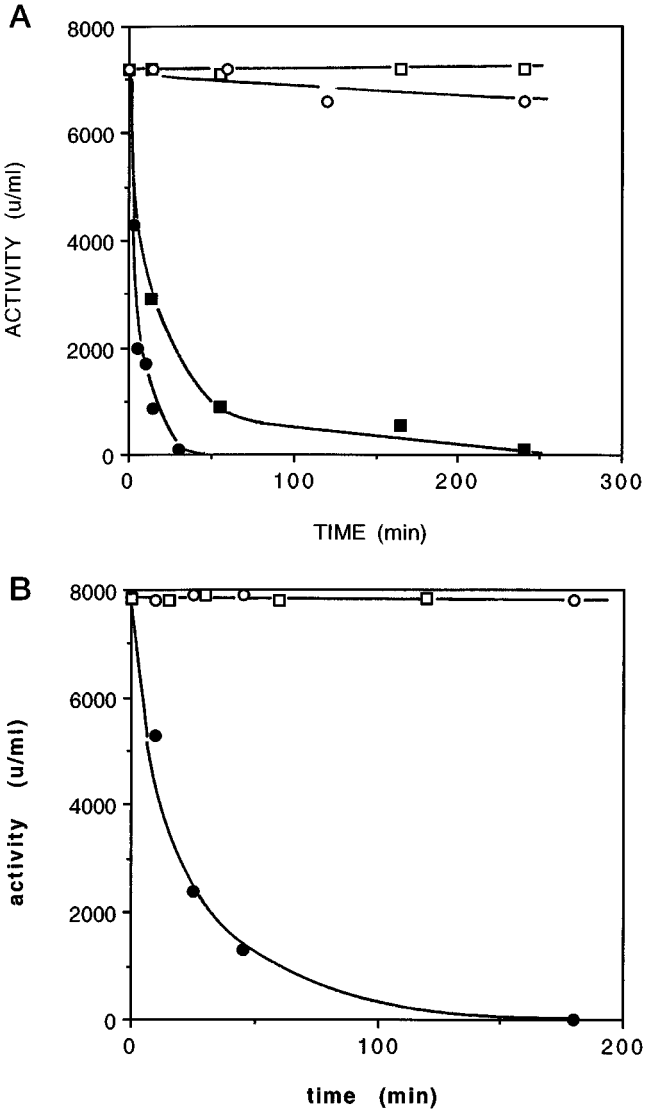

FIG. 9. **Influence of nonionic detergent concentrations on lipase inhibition by E600 in the presence of colipase.** Porcine lipase (1.4×10^{-5} M) was incubated at pH 6.0 with 4 mM E600 in the presence of colipase (4.2×10^{-5} M) and various TGME or βOG concentrations. *A*, 1.5 mM (□), 4.5 mM (○), 7.5 mM (■), and 15 mM (●) of TGME. *B*, 5 mM (□); 15 mM (○), and 25 mM (●]) of βoG. At different periods of time, aliquots were withdrawn from the incubation mixture, and the remaining lipase activity was determined at pH 7.5 as described under "Experimental Procedures." The activity was expressed as units/ml of the lipase stock solution.

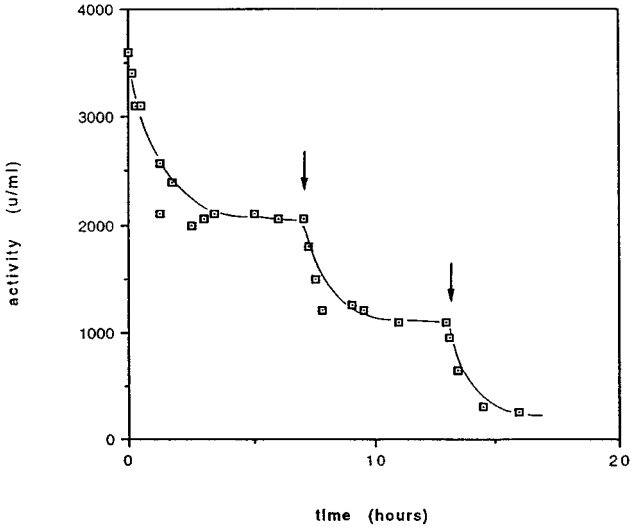

FIG. 10. **Influence of the colipase/lipase molar ratio on the E600 inhibition of lipase in the presence of a supramicellar concentration of TGME.** Porcine lipase (3.5×10^{-5} M) and colipase (1.7×10^{-5} M) were incubated with 4 mM E600. The *arrows* indicate the two subsequent additions of 0.85 10^{-5} M colipase.

In the presence of colipase, a shift of the inhibitory effects toward higher detergent concentrations was observed for both ionic and nonionic surfactants. However, a major difference was observed between the effects of NaTDC (Fig. 11*A*) and those of the two nonionic detergents (Fig. 11, *B* and *C*). As it has been well documented, colipase was capable of reversing the inhibitory effect of NaTDC. In contrast, it failed to restore the lipase activity abolished by either TGME or βoG.

DISCUSSION

This work describes the three-dimensional structure of the first natural lipase-colipase (porcine) complex as determined by x-ray crystallography. The complex contains the third three-dimensional structure to be determined for a pancreatic lipase. As expected from the high degree of amino acid sequence homology, the porcine lipase structure is very similar to the corresponding human (17, 18, 22) and horse (19) enzymes. The porcine and human lipases are glycosylated at Asn^{167}. Although significant electron density was observed in this region for the human enzyme, no glycan structure was reported (55). In the porcine enzyme the first five sugar residues are relatively well ordered and could be built into the electron density. The glycosylation site is remote from the active site, and the carbohydrate chain is unlikely to play a role in catalysis.

The structures of the porcine lipase-porcine colipase and the human lipase-porcine colipase complexes (22) are similar. An optimal superposition of the lipase C-terminal domains of both complexes results in a very good agreement not only for the positions of these domains, but also for the position of the flap regions and the colipase molecules. In consequence, the eight lipase-colipase polar interactions observed in the human-porcine complex are also observed in the porcine complex. This conservation results from the fact that nearly all the residues that interact through their side chains are invariant and that the two amino acids that are not (Leu^{16} from colipase and Val^{247} from lipase) interact through their main chain atoms only. This certainly explains why colipases from various species can restore the activity of the different lipases in the presence of bile salts. There is one exception to the conservation of lipase-colipase interactions: the human-porcine complex displays a salt bridge between Asp^{390} (lipase) and Arg^{44} (colipase) that does not exist in the natural porcine complex, although both residues are conserved. Furthermore, this bridge could not form in the natural human complex, where Arg^{44} is substituted by Ser. In the uncomplexed human lipase Asp^{390} forms a salt bridge with Lys^{367} (Fig. 3).[3] Although such bridging contact should be conserved in the human natural complex, it has been broken in the human-porcine complex presumably because of the more favorable double interaction of Asp^{390} with Arg^{44} (Fig. 3). In the porcine complex, Asp^{390} interacts with Arg^{368}, whereas Arg^{44} of colipase is involved in two water-mediated interactions with Asn^{366} of lipase. These interactions may be strong enough to preclude formation of the salt bridge between Asp^{390} and Arg^{44}. Because the pH of crystallization is very similar in the two cases, it is unlikely that the differences are due to variations in residue charges. Arg^{386} also forms a salt bridge with Asp^{390} in the uncomplexed equine enzyme (19).

Lipase presents an intrinsic flexibility in the relative posi-

[3] F. Winkler, personal communication.

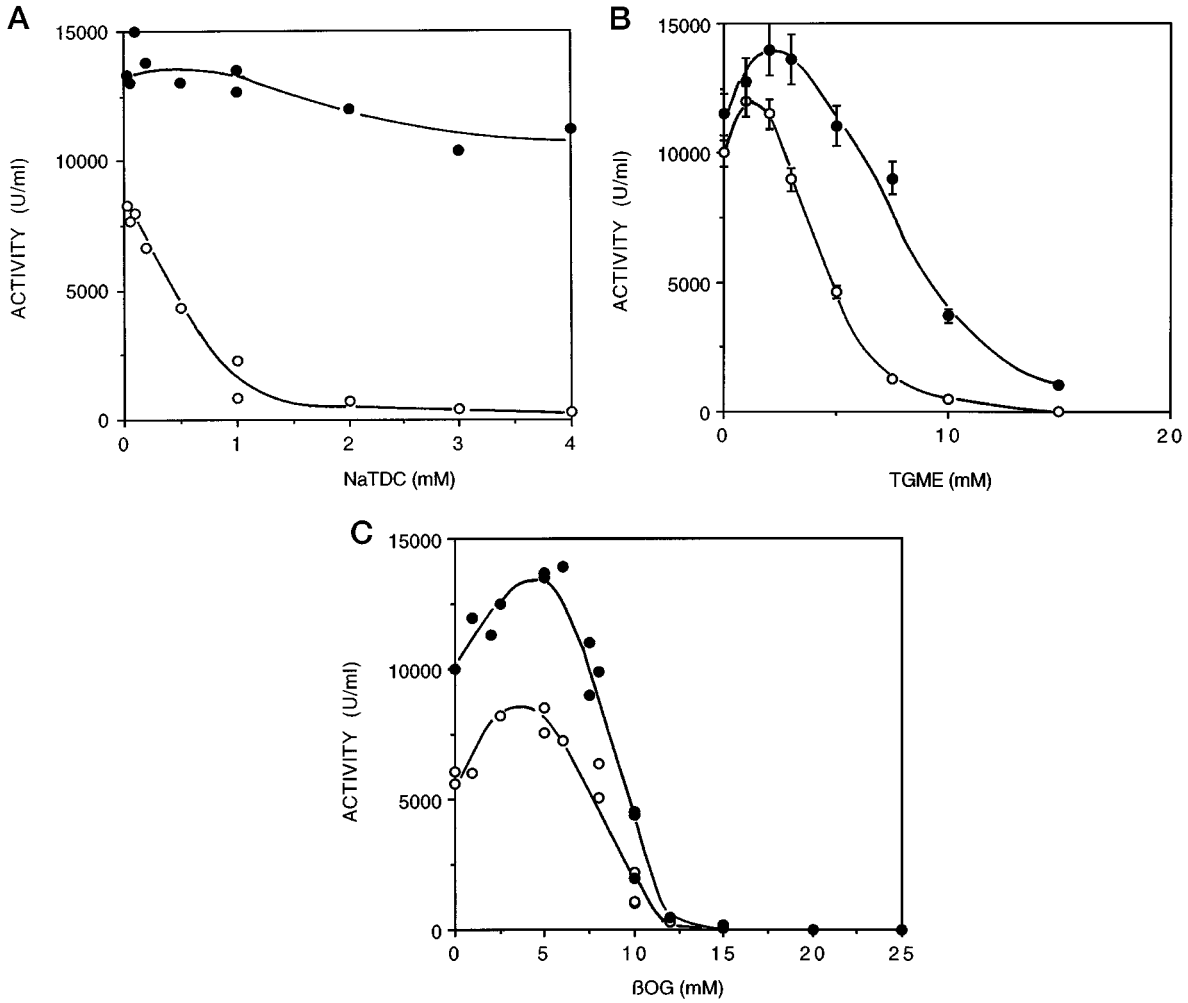

FIG. 11. **Porcine pancreatic lipase activity as a function of detergent concentration.** The influence of NaTDC (*A*), TGME (*B*), and βoG (*C*) on lipase activity was tested at pH 7.5 using emulsified tributyrin as indicated in the text. The experiments were performed either in the absence (○) or in the presence (●) of a three-molar excess of porcine colipase. The activity was expressed as units/ml of the lipase stock solution. For *A* and *C*, all the experimental points are represented. For *B*, *error bars* are indicated.

tion of its N- and C-terminal domains, as indicated by the small rotation around residues 334–335, detected when comparing the porcine and human-porcine complexes. This property of the N-terminal domain to move independently from the flap, colipase, and the C-terminal domain may have functional implications as the lipase molecule binds the water-lipid interface.

In the crystalline natural complex the porcine lipase is in the open state, suggesting that nonionic detergent micelles are able to activate the enzyme in the presence of colipase. In solution, this has been clearly demonstrated by the inhibition of lipase by E600, a consequence of the opening of the flap by the combined effect of colipase and detergent micelles. This activation, which does not require the presence of substrate, can be induced both by ionic detergents such as NaTDC and nonionic detergents such as TGME and βoG. The opening of the flap is a reversible phenomenon because decreasing the detergent concentration below the critical micellar concentration by dialysis prevents E600 inhibition, indicating that lipase reverts to a closed conformation, even in the presence of colipase.

These experiments strongly suggest that the open conformation found in the porcine complex crystal structure was induced by pure detergent micelles and not by artefactual crystallizations effects. Whether detergent micelles are present in our crystals is not known, although they might be lodged in the large channels (35 Å in diameter) formed by the crystal packing. This, in turn, would explain the reasonably good diffracting power for crystals with an estimated solvent content of 70%.

Once the flap opens, the active site becomes accessible to reagents (such as E600), competitive inhibitors, and substrates. In the porcine lipase colipase complex, the substrate binding canyon is occupied by one TGME molecule that displays two discreet conformations. Stabilization of this molecule results from 1) the possibility for the aliphatic region of the detergent molecule to adapt to the hydrophobic substrate binding site of lipase and 2) polar interactions of O-16 with Ser^{153} of the catalytic triad for conformer 1 and with Gly^{77} and Trp^{86} for conformer 2. The latter two residues, which are conserved in all known lipase sequences, may be part of the recognition site for the triglyceride molecule, a notion that could be tested by site-directed mutagenesis. In addition, TGME monomer binding to the active site may explain the observed inhibitory effect of the detergent on enzymatic triglyceride hydrolysis at concentrations well below the critical micellar concentration. Because this effect was also observed for βoG, nonionic detergents in general are likely to be inhibitors of lipase. In contrast to the inhibition induced by bile salts, nonionic detergent inhibition cannot be reversed by colipase. At this time, we do not have an explanation for this phenomenon.

Our results are consistent with the conformation of the human lipase crystal structure as determined by Winkler *et al.* (17). Although in principle micelles of βoG were used in their

crystallization experiments, the absence of colipase led to a closed conformation of the enzyme. van Tilbeurgh *et al.* (22) have proposed that the opening of the flap in their human-porcine crystalline complex was induced by the presence of mixed micelles made of phospholipids and bile salts. Their conclusion was based on the fact that a previous crystallographic analysis of the human-porcine complex carried out in the absence of mixed micelles but in the presence of supramicellar concentrations of βoG (56) resulted in a closed lipase flap conformation (18). Other factors must have influenced the flap conformations in that study, because our results indicate that micelles of βoG alone, a detergent used in their crystallization mixture, are capable of inducing the opening of the lipase flap in solution. In this respect, one intriguing observation is that in the three known lipase-colipase complexes (18, 22, 23), the active site is occupied either by a subtrate analog or by an inhibitor. It may very well be that in addition to micelles, the colipase-lipase complex requires the presence of a molecule bound to the active site in order to crystallize under the open form.

In summary, the results presented here shed new light on the understanding of the process of pancreatic lipase activation. They clearly demonstrate that the presence of micelles of either ionic or nonionic detergents plus colipase induces the opening of the flap. They also show, by superposition of the human-porcine and porcine complexes, that the N-terminal domain, except for the flap region, behaves like a rigid body that can swing relative to the rest of the molecule. This, in turn, suggests that binding to the water-lipid interphase may require a certain degree of conformational flexibility. In addition, the determination of the three-dimensional structure of the natural porcine lipase-colipase complex has allow us to establish, by comparison with the human-porcine complex, the minimal set of interactions required for complex formation. Finally, the presence of a TGME molecule in the lipase active site provides a structural basis for the inhibitory effect of the detergent. This may be a general phenomenon, implying that once the flap is opened, either by the water-substrate interface or by detergent micelles in the presence of colipase, monomers of nonionic detergents may behave as inhibitors by binding to the active site. The availability of a simple lipase-activating system, corresponding to homogeneous detergent micelles, should be instrumental in the study of the activation mechanism of these enzymes.

Acknowledgments—We thank E. Foglizzo for skillful assistance in the biochemical part of this work. We also thank Christine Gaboriaud and Dominique Housset for stimulating discussions and R. Fourme and J. P. Benoit for help with data collection at Laboratoire pour l'Utilisation du Rayonnement Electromagnetique (Orsay, France).

REFERENCES

1. Borgström, B. & Erlanson, C. (1973) *Eur. J. Biochem.* **37,** 60–68
2. Chapus, C., Sari, H., Sémériva, M. & Desnuelle, P. (1975) *FEBS Lett.* **58,** 155–158
3. Vandermeers, A., Vandermeers-Piret, M. C., Rathé, S. & Christophe, J. (1975) *FEBS Lett.* **49,** 334–337
4. De Caro, J., Boudouard, M., Bonicel, J., Guidoni, A., Desnuelle, P. & Rovery, M. (1981) *Biochim. Biophys. Acta* **671,** 129–138
5. Lowe, M. E., Rosenblum, J. L. & Strauss, W. A. (1989) *J. Biol. Chem.* **264,** 20042–20048
6. Kerfelec, B., Foglizzo, E., Bonicel, J., Bougis, P. E. & Chapus, C. (1992) *Eur. J. Biochem.* **206,** 279–287
7. Aleman-Gomez, J. A., Colwell, N. C., Sasser, T. L. & Kumar, V. B. (1992) *Biochem. Biophys. Res. Commun.* **188,** 964–971
8. Sims, H. F., Strauss, A. W. & Lowe, M. E. (1992) *Genbank* M–58369
9. Carrière, F., Thirstrup, K., Hjorth, S. & Boel, E. (1994) *FEBS Lett.* **338,** 63–68
10. Thirstrup, K., Carrière, F., Hjorth, S. A., Rasmussen, P. B., Nielsen, P. F., Ladefoged, C., Thim, L. & Boel, E. (1995) *Eur. J. Biochem.* **227,** 186–193
11. Kerfelec, B., LaForge, K. S., Puigserver, A. & Scheele, G. (1986) *Pancreas* **1,** 430–437
12. Wishart, M., Andrews, P., Nichols, R., Blevine, G., Logsdon, C. & Williams, J. (1993) *J. Biol. Chem.* **268,** 10303–10311
13. Payne, R. M., Sims, H. F., Jennens, M. L. & Lowe, M. E. (1994) *Am. J. Physiol.* **266,** G914–G921
14. Giller, T., Buchwald, P., Blum-Kaelin, D. & Hunziker, W. (1992) *J. Biol. Chem.* **267,** 16509–16516
15. Hjorth, A., Carrière, F., Cudrey, C., Woldike, H., Boel, E., Lawson, D., Ferrato, F., Cambillau, C., Dodson, G., Thim, L. & Verger, R. (1993) *Biochemistry* **32,** 4702–4707
16. Thirstrup, K., Verger, R. & Carrière, F. (1994) *Biochemistry* **33,** 2748–2756
17. Winkler, F. K., D'Arcy, A. & Hunziker, W. (1990) *Nature* **343,** 771–774
18. van Tilbeurgh, H., Sarda, L., Verger, R. & Cambillau, C. (1992) *Nature* **359,** 159–162
19. Bourne, Y., Martinez, C., Kerfelec, B., Lombardo, D., Chapus, C. & Cambillau, C. (1994) *J. Mol. Biol.* **238,** 709–732
20. Mahe-Gouhier, N. & Léger, C. (1988) *Biochim. Biophys. Acta* **962,** 91–97
21. Abousalham, A., Chaillan, C., Kerfelec, B., Foglizzo, E. & Chapus, C. (1992) *Protein Eng.* **5,** 105–111
22. van Tilbeurgh, H., Egloff, M.-P., Martinez, C., Rugani, N., Verger, R. & Cambillau, C. (1993) *Nature* **362,** 814–820
23. Egloff, M. P., Marguet, F., Buono, G., Verger, R., Cambillau, C. & van Tilbeurgh, H. (1995) *Biochemistry* **34,** 2751–2762
24. Egloff, M. P., Sarda, L., Verger, R., Cambillau, C. & van Tilbeurgh, H. (1995) *Protein Sci.* **4,** 44–57
25. Charles, M., Erlanson, C., Bianchetta, J., Joffre, J., Guidoni, A. & Rovery, M. (1974) *Biochim. Biophys. Acta* **359,** 186–197
26. Crenon, I., Granon, S., Chapus, C. & Kerfelec, B. (1994) *Biochim. Biophys. Acta* **1213,** 357–360
27. Wicker, C. & Puigserver, A. (1990) *Biochem. Biophys. Res. Commun.* **167,** 130–136
28. Fukuoka, S. I., Taniguchi, Y., Kitagawa, Y. & Scheele, G. (1990) *Nucleic Acids Res.* **18,** 5549
29. Colwell, N. C., Aleman-Gomez, J. A., Sasser, T. L. & Kumar, V. B. (1992) *Genbank* L–06329
30. Granon, S. (1986) *Biochim. Biophys. Acta* **874,** 54–60
31. Erlanson, C., Barrowman, J. A. & Borgström, B. (1977) *Biochim. Biophys. Acta* **489,** 150–162
32. Chaillan, C., Rogalska, E., Chapus, C. & Lombardo, D. (1989) *FEBS Lett.* **257,** 443–446
33. Lombardo, D., Chapus, C., Bourne, Y. & Cambillau, C. (1989) *J. Mol. Biol.* **205,** 259–261
34. Chapus, C., Desnuelle, P. & Foglizzo, E. (1981) *Eur. J. Biochem.* **115,** 99–105
35. Mc Pherson, A. (1985) *Methods Enzymol.* **114,** 112–120
36. Howard, A. J., Gilliland, G. L., Finzel, B. C., Poulos, T. L., Ohlendorf, D. H. & Salemme, F. R. (1987) *J. Appl. Crystallogr.* **20,** 383–387
37. Leslie, A. G. W. (1987) in *Computational Aspects of Protein Crystal Data Analysis* (Helliwell, J. H., Machin, P. A. & Papiz, M. Z., eds) pp. 39–50, Proceedings of the Daresbury Study Weekend, 23–24 January, 1987
38. Matthews, B. W. (1968) *J. Mol. Biol.* **33,** 491–497
39. CCP4 (1979) *The S.E.R.C. (U.K.) Collaborative Computing Project No. 4, A Suite of Programs for Protein Crystallography*, Daresbury Laboratory, Warrington WA4 4AD, UK
40. Navaza, J. (1994) *Acta Crystallogr. Sect. B Struct. Sci.* **50,** 157–163, and references therein
41. Castellano, E., Olivia, G. & Navaza, J. (1992) *J. Appl. Crystallogr.* **25,** 281–284
42. Jones, T. A., Zou, J.-Y., Cowan, S. W. & Kjeldgaard, M. (1991) *Acta Crystallogr. Sect. B Struct. Sci.* **47,** 110–119
43. Brünger, A. T. (1988) in *Crystallographic Computing 4: Techniques and Technologies* (Isaac, N. W. & Taylor, M. R., eds) pp. 126–140, Clarendon Press, Oxford
44. Charles, M., Erlanson, C., Bianchette, J., Joffre, J., Guidoni, A. & Rovery, M. (1974) *Biochim. Biophys. Acta* **359,** 186–197
45. Chothia, C. & Janin, J. (1982) *Biochemistry* **21,** 3955–3965
46. Garner, C. W. & Smith, L. C. (1972) *J. Biol. Chem.* **247,** 561–565
47. De Caro, A., Figarella, C., Amic, J., Michel, R. & Guy, O. (1977) *Biochim. Biophys. Acta* **490,** 411–419
48. Fournet, B., Leroy, Y., Montreuil, J., De Caro, J., Rovery, M., van Kuik, A. & Vliegenthart, F. G. (1987) *Eur. J. Biochem.* **170,** 369–371
49. Plummer, T. H. & Sarda, L. (1973) *J. Biol. Chem.* **248,** 7865–7869
50. Benkouka, F., Guidoni, A., De Caro, J., Bonicel, J., Desnuelle, P. & Rovery, M. (1982) *Eur. J. Biochem.* **128,** 331–341
51. Verger, R., Sarda, L. & Desnuelle, P. (1971) *Biochim. Biophys. Acta* **242,** 580–592
52. Maylie, M. F., Charles, M. & Desnuelle, P. (1972) *Biochim. Biophys. Acta* **276,** 162–175
53. Guidoni, A., Benkouka, F., De Caro, J. & Rovery, M. (1981) *Biochim. Biophys. Acta* **660,** 148–150
54. Börgstrom, B. (1977) *Biochim. Biophys. Acta* **488,** 381–391
55. Winkler, F. K. & Gubernator, K. (1994) in *Lipases, Their Structure, Biochemistry and Application* (Woolley, P. & Petersen, S. B., eds) pp. 139–159, Cambridge University Press, Cambridge, UK
56. van Tilbeurgh, H., Gargouri, Y., Dezan, C., Egloff, M. P., Nesa, M. P., Rugani, N., Sarda, L., Verger, R. & Cambillau, C. (1993) *J. Mol. Biol.* **229,** 552–554
57. Kraulis, P. J. (1991) *J. Appl. Crystallogr.* **24,** 946–950
58. Nicholls, A., Sharp, K. & Honig, B. (1991) *Proteins Struct. Funct. Genet.* **11,** 281
59. Ligplot. Andrew Wallace; Biomolecular Structure and Modelling Unit. Dept. of Biochemistry, University College, Gower Street, London WC1E 6BT, England